Estimation of Illuminant Direction and Intensity of Multiple Light Sources

Wei Zhou and Chandra Kambhamettu

Video/Image Modeling and Synthesis (VIMS) Lab
Department of Computer and Information Sciences
University of Delaware, Newark DE 19716, USA,
wzhou,chandra@cis.udel.edu,
http://www.cis.udel.edu/~wzhou/research/research.html
http://www.cis.udel.edu/~vims

Abstract. This paper presents a novel scheme for locating multiple light sources and estimating their intensities from a pair of stereo images of a sphere. No prior knowledge of the location and radius of the sphere is necessary. The sphere surface is not assumed to be a pure Lambertian surface, instead, it has both Lambertian and specular properties. The light source locating algorithm is based on the fact that the Lambertian intensity is not dependent on the direction of view point, while the specular intensity is highly dependent on the direction of the view point. From this fact, we can use a pair of stereo images whose view point changes can be utilized to separate the image of the sphere into two images, one with Lambertian intensities, and the other with specular intensities. The specular image is used to find the directions of the light sources, and then Lambertian image model is used to find the intensities of the light sources. Experiments on both synthetic and real images show that the scheme is successful and robust in finding the directions of the light sources accurately with accurate intensity estimation.

1 Introduction

Light source location information is an important issue for both computer vision and computer graphics applications. For example, shape from shading algorithms [1] [2] [5] need the light source directions as a prior knowledge, segmentation algorithms can be improved if we know the information about the illumination source [15], and we can combine synthetic imagery with a real scene in a seamless manner if the illumination information is available.

The works in estimating light source direction can be traced back to the work of Pentland [9] in the early 1980's. Since then, many schemes have been proposed in the context of shape from shading [5] [6] [2] [3] [4], where a point source that is far away is assumed. Multiple light sources detection is more challenging, and there are relatively few papers dealing with such a problem. In [13], Yang

A. Heyden et al. (Eds.): ECCV 2002, LNCS 2353, pp. 206–220, 2002.

and Yuille show that information on the occluding boundary imposes strong constrains on the light source direction. In [11], Hougen and Ahuja use the least squares technique to solve the multiple light source problem. But as [13] pointed out, without any extra information, estimating light sources from a single image is a highly ill-posed problem. Recently, many researchers have tried to extract illumination information from a single image together with other information, such as the shape of the object in question. In [7], Yufei and Yee-Hong use the image of a sphere of known size, where Lambertian surface and directional light sources are assumed. In real world, since the intensities of an object always contains both specular and diffuse intensities and the size of the object is always unknown, the assumption of pure Lambertian surface and known size of the sphere restricts its applications. In [14] [15], two or three spheres are used, and the specular properties of a shining surface is used to triangulate the locations of light sources. Since it only uses the specular information, the intensities of the light sources can not be estimated.

In this paper, our goal is similar to that of [7], i.e, estimating the intensities and directions of light sources. Like [7], we also use a sphere, but no prior knowledge about the sphere such as the radius and the center is necessary. The radius and center of the sphere are calculated from a pair of stereo images of the sphere, based on the geometry relations of the projected sphere boundaries with the sphere center and radius. Also the Lambertian surface of the sphere is not assumed, instead, we consider that the intensities of the sphere surface may contain both Lambertian and specular intensities, and a simple algorithm is proposed to separate the Lambertian intensities from the specular intensities. The specular information is used to find the directions of the light sources, and the Lambertian information is used to estimate the intensities of the light sources.

The paper is organized as follows. In section 2.1, we introduce a way to calculate the center location and radius of the sphere from a pair of stereo images of the sphere. In section 2.2, we study how to generate the Lambertian and specular images based on the point correspondences imposed by the 3-d structure of the sphere. Algorithms are proposed in section 2.3 and 2.4 to get the directions and intensities of light sources using the specular image and the Lambertian image respectively. In section 3, we present experimental results obtained from both synthetic images and real images to show that the proposed algorithm can find the directions of the light sources accurately with accurate intensity estimation.

2 Methodology

2.1 Finding the Center and Radius of the Sphere

In our framework, images are taken by a pair of well calibrated stereo cameras with known focal length and baseline, and the object in the image is a sphere whose surface has both Lambertian and specular properties. We assume the perspective projection and that the left camera (projection reference point) is sitting on the origin $(0, 0, 0)$ of the xyz-space, so the right camera is sitting on

the $(b, 0, 0)$, where b is the baseline. The direction of the cameras is the positive z-axis. Each light direction is represented in the xyz-space as (lx_i, ly_i, lz_i). Figure 1a illustrates the coordinate system.

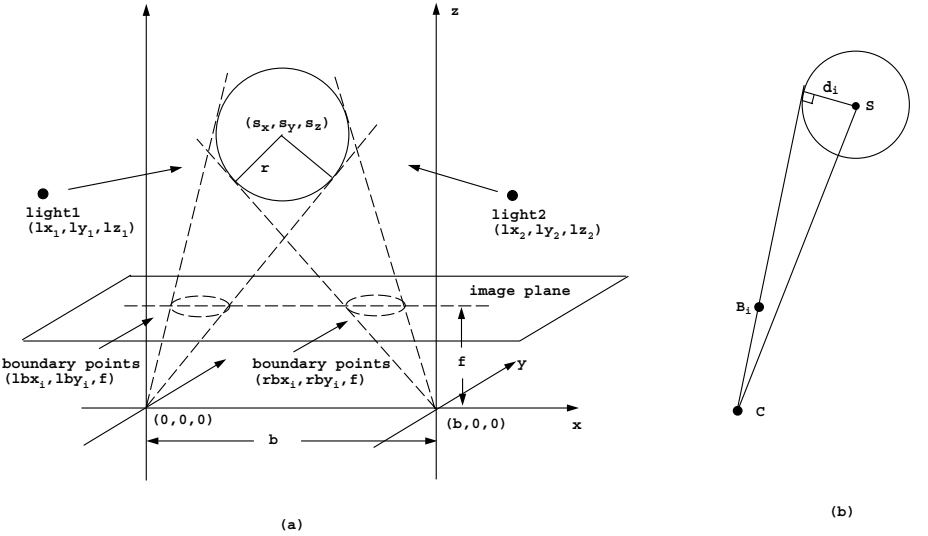

Fig. 1. Imaging coordinates system

There are two facts about the perspective image of a sphere:

1. the line passing through the camera center and any boundary point of the sphere in the image plane is a tangent line to the sphere;
2. the perpendicular distance from the center of the sphere to a tangent line of the sphere is the radius of the sphere.

Suppose the center of the sphere is located at (s_x, s_y, s_z), and the radius is r. The boundary points in the left image are represented as (lbx_i, lby_i, f), and similarly, the boundary points in the right image are represented as (rbx_i, rby_i, f), where f is the focal length. From Figure 1b, we know that the distance d_i from the sphere center S to the line passing through any boundary point B_i and the camera center C is:

$$d_i^2 = \|\boldsymbol{CS}\|^2 - \left(\frac{\boldsymbol{CS} \cdot \boldsymbol{CB_i}}{\|\boldsymbol{CB_i}\|}\right)^2. \tag{1}$$

Then, for the boundary points in the left and right images, we get:

$$ld_i^2 = \|(s_x, s_y, s_z)\|^2 - \left(\frac{(s_x, s_y, s_z) \cdot (lbx_i, lby_i, f)}{\|(lbx_i, lby_i, f)\|}\right)^2 \tag{2}$$

$$rd_i^2 = \|(s_x - b, s_y, s_z)\|^2 - \left(\frac{(s_x - b, s_y, s_z) \cdot (rbx_i - b, rby_i, f)}{\|(rbx_i - b, rby_i, f)\|}\right)^2 \tag{3}$$

where ld_i and rd_i are the distances calculated using the boundary points in the left and right image respectively.

Using boundary tracking algorithm, the boundary points of the sphere can be easily detected. Since the focal length f and baseline b are all known, the distances ld_i and rd_i only depend on the location of the sphere center (s_x, s_y, s_z), and so can be written as functions of these three unknowns:

$$ld_i^2 = h_i(s_x, s_y, s_z) \tag{4}$$

$$rd_i^2 = g_i(s_x, s_y, s_z). \tag{5}$$

Based on the fact (2), we can define two error functions:

$$EOF_1 = \sum_{i=1}^{m} (h_i(s_x, s_y, s_z) - r^2)^2 \tag{6}$$

$$EOF_2 = \sum_{i=1}^{n} (g_i(s_x, s_y, s_z) - r^2)^2. \tag{7}$$

Minimizing the two error functions above gives us two relations between the sphere center and the radius, and from these two relations, we can get the location of the sphere center and the radius.

2.2 Separating the Images

Assuming that the distances between the light sources and every point on the sphere surface are large enough compared to the radius of the sphere, and the sphere surface has uniform reflection properties, the intensity of a point on the sphere surface can be written as:

$$I = I_{ambient} + \sum_{i=1}^{n} (I_{diffuse}^{(i)} + I_{specular}^{(i)}) \tag{8}$$

where $I_{ambient}$ represents the ambient intensity, $I_{diffuse}^{(i)}$ and $I_{specular}^{(i)}$ represent the diffuse and specular intensity contributed by the i'th light source respectively.

There are two observations in the illumination and stereo imaging:

1. The ambient and diffuse intensities are independent of view direction, while specular intensity is highly dependent on the view direction.
2. Only difference between the stereo image pairs is the changed view direction.

Based on these two observations, intensities of the stereo image pair can be compared to separate the specular intensity from the diffuse and ambient intensities. Since we already obtained the center and radius of the sphere (presented in the last section), a sphere model in the 3-d space can be created, and the 3-d position of each point on the sphere surface can be determined uniquely. Projecting a 3-d point on the sphere surface onto the left and right image planes gives us two image pixels. Apparently, these two image pixels correspond to the

same 3-d point - thus, we can establish a pixel correspondences table between the two stereo images. Suppose that pixel (i_1, j_1) in the left image corresponds to pixel (i_2, j_2) in the right image, from the first observation we have:

$$I_{ambient}(i_1, j_1) = I_{ambient}(i_2, j_2) \tag{9}$$

$$I^{(i)}_{diffuse}(i_1, j_1) = I^{(i)}_{diffuse}(i_2, j_2). \tag{10}$$

The intensity difference between these two pixels is:

$$\begin{aligned} D(i_1, j_1, i_2, j_2) &= I(i_1, j_1) - I(i_2, j_2) \\ &= I_{ambient}(i_1, j_1) + \sum_{i=1}^{n} (I^{(i)}_{diffuse}(i_1, j_1) + I^{(i)}_{specular}(i_1, j_1)) \\ &- I_{ambient}(i_2, j_2) - \sum_{i=1}^{n} (I^{(i)}_{diffuse}(i_2, j_2) + I^{(i)}_{specular}(i_2, j_2)) \\ &= \sum_{i=1}^{n} (I^{(i)}_{specular}(i_1, j_1) - I^{(i)}_{specular}(i_2, j_2)). \end{aligned} \tag{11}$$

Let

$$D^{(i)}(i_1, j_1, i_2, j_2) = I^{(i)}_{specular}(i_1, j_1) - I^{(i)}_{specular}(i_2, j_2), \tag{12}$$

then

$$D(i_1, j_1, i_2, j_2) = \sum_{i=1}^{n} D^{(i)}(i_1, j_1, i_2, j_2). \tag{13}$$

From above formula, we know that the intensity difference $D(i_1, j_1, i_2, j_2)$ only depends on the specular intensities. Based on Phong specular-reflection model [12] and using notations shown in figure 2, we have:

$$I^{(i)}_{specular}(i_1, j_1) = Is^{(i)}(cos\theta_1)^{n_s} \tag{14}$$

$$I^{(i)}_{specular}(i_2, j_2) = Is^{(i)}(cos\theta_2)^{n_s} \tag{15}$$

$$\theta_1 + \theta_2 \geq \alpha \tag{16}$$

where $Is^{(i)}$ is a constant representing the maximum specular intensity contributed by the i'th light source, n_s is the specular-reflection parameter, θ_1 is the angle between view vector V_1 and reflect vector R, θ_2 is the angle between view vector V_2 and R, and α is the angle between two view vectors V_1 and V_2.

If n_s and α are large enough, i.e, if the sphere is shing and the baseline is large enough, we can define a small number $\epsilon < \alpha/2$, such that:

$$(cos\theta)^{n_s} \approx \begin{cases} 1 \text{ if } \theta < \epsilon \\ 0 \text{ otherwise.} \end{cases}$$

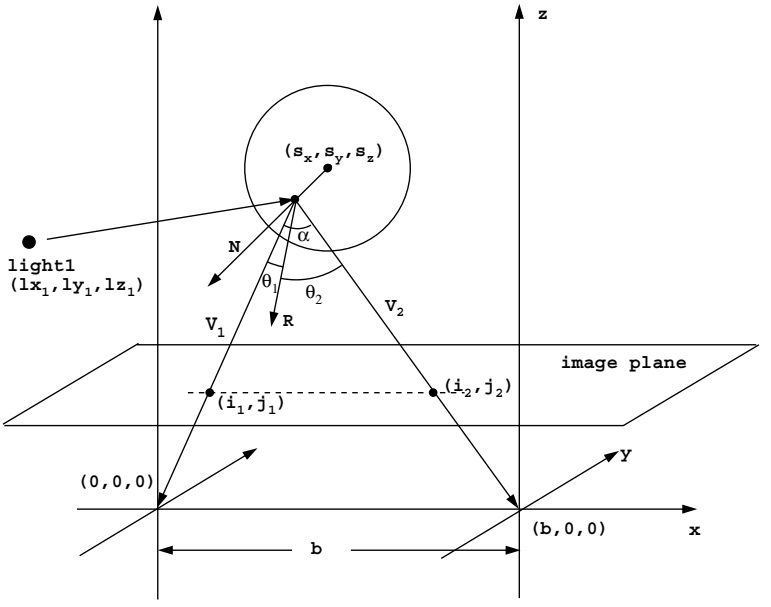

Fig. 2. Specular imaging configuration

Then, we have:

$$I^{(i)}_{specular}(i_1, j_1) \approx \begin{cases} I^{(i)}_s \text{ if } \theta_1 < \epsilon \\ 0 \quad \text{otherwise} \end{cases} \tag{17}$$

and

$$I^{(i)}_{specular}(i_2, j_2) \approx \begin{cases} I^{(i)}_s \text{ if } \theta_2 < \epsilon \\ 0 \quad \text{otherwise} \end{cases} \tag{18}$$

From equation(16), we know that θ_1 and θ_2 can not be less than ϵ at the same time, this means that $I^{(i)}_{specular}(i_1, j_1)$ and $I^{(i)}_{specular}(i_2, j_2)$ can not both equal to $I^{(i)}_s$ at the same time. So we can deduce:

if $D^{(i)}(i_1, j_1, i_2, j_2) = 0$, then:

$$I^{(i)}_{specular}(i_1, j_1) = 0 \; and \; I^{(i)}_{specular}(i_2, j_2) = 0 \tag{19}$$

otherwise:

$$I^{(i)}_{specular}(i_1, j_1) = I^{(i)}_s \; or \; I^{(i)}_{specular}(i_2, j_2) = I^{(i)}_s. \tag{20}$$

Assuming that the light sources are not very clustered, i.e $D^{(i)}(i_1, j_1, i_2, j_2)$ will not interfere with each other, $D(i_1, j_1, i_2, j_2)$, the sum of all intensity differences, would have the same properties as $D^{(i)}(i_1, j_1, i_2, j_2)$, any individual intensity difference. We define two thresholds $th_{diffuse}$ and $th_{specular}$, when

$D(i_1, j_1, i_2, j_2)$ is less than $th_{diffuse}$, the specular component of the intensity of the pixel would be so small that the intensity of the pixel only contains diffuse and ambient components. We call these pixels Lambertian pixels, and the image that contains only lamberetian pixels as Lambertian image. When $D(i_1, j_1, i_2, j_2)$ is larger than $th_{specular}$, the specular component should be large, and we call these pixels specular pixels, and the image that contains only specular pixels the specular image. Figure 3 illustrate the separation of the image.

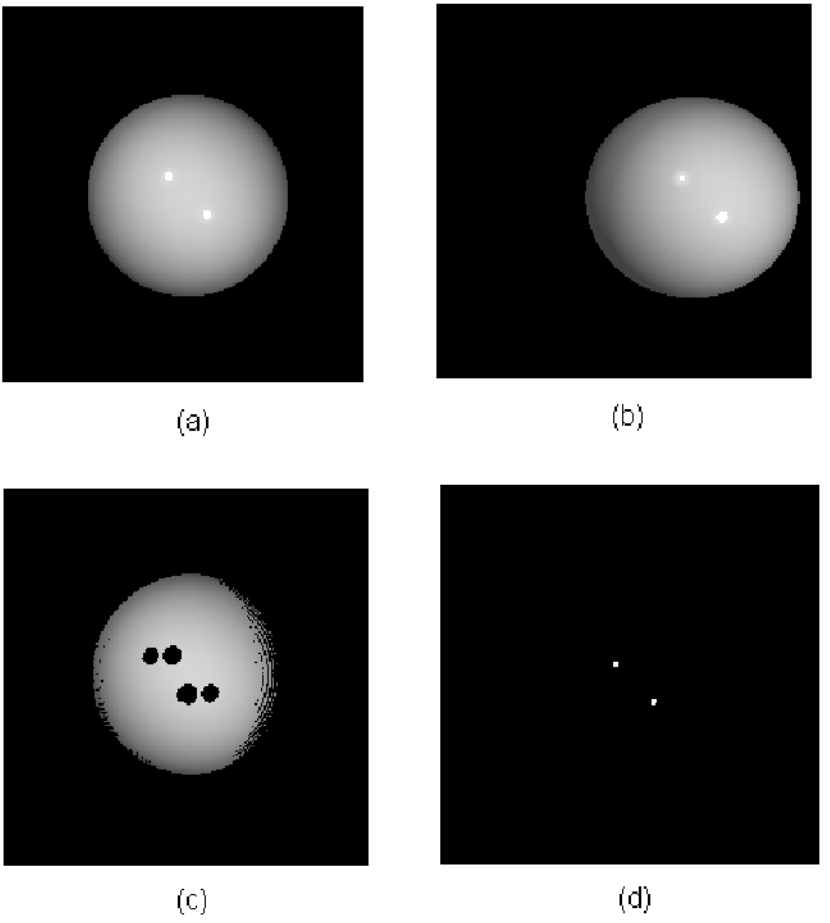

Fig. 3. Separation of image (a) initial right image (b) initial left image (c) Lambertian image (d) specular image

2.3 Estimation of Directions of Light Sources

The specular reflection has a property that at a specular point on a surface, the angle of incoming light from the illuminant and the angle of outgoing light to the camera are equal. In the last section, we have already generated the specular image pair of the sphere which only contains the specular spots. Each spot correspond to a light source, and each light source will produce a specular spot in each image. The locations of these two corresponding specular spots are determined and used for the calculation of the direction of the light source.

The correspondence of the specular spots between two specular images is easy to establish. Similar to [14], we can determine which pairs of spots result from the same illuminant by grouping the specular spots by their relative locations. In our implementation, we sort the specular spots first by their horizontal coordinates and then by their vertical coordinates for each image, which effectively pairs the specular spots together.

One problem in locating the specular spot is that the specular spot is a region which contains many pixels, and we must find a pixel inside it to represent this region. One natural way is using the centroid point of the region.

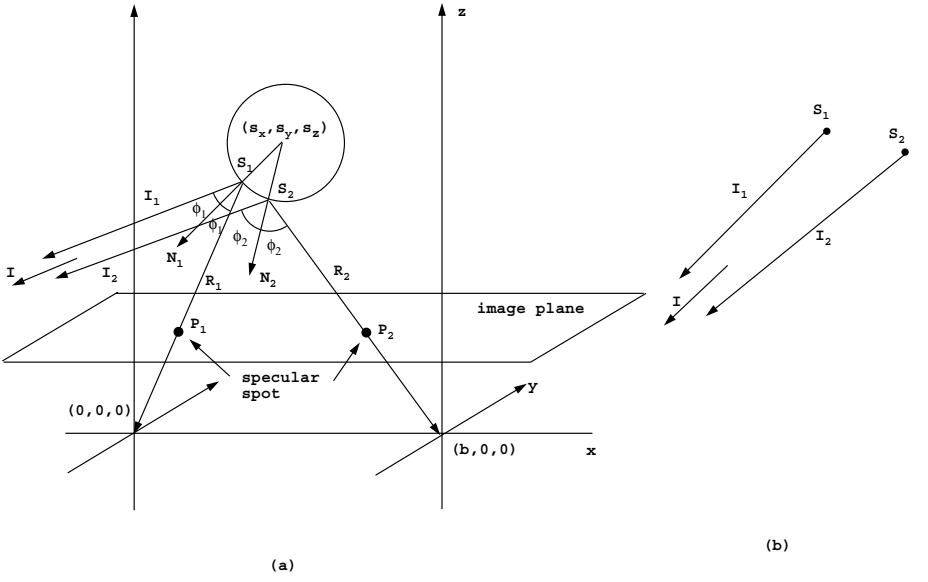

Fig. 4. Specular imaging geometry

Figure 4a illustrates the imaging geometry. P_1 and P_2 are the specular pixels in the left and the right images resulting from the same illuminant I, S_1 and S_2 are the corresponding points of P_1 and P_2 on the sphere surface. Once we know the locations of P_1 and P_2, S_1 and S_2 can be determined, then normal vectors N_1, N_2 and reflection vectors R_1, R_2 can be calculated. The illuminant direction

vector I_1 and I_2 can be calculated according to the specular reflection property:

$$I_1 = (2N_1 \cdot R_1)N_1 - R_1 \tag{21}$$

$$I_2 = (2N_2 \cdot R_2)N_2 - R_2. \tag{22}$$

Ideally, I_1, I_2 should be equal to I. Here, we use the average of I_1 and I_2 to get I in order to eliminate noise. Thus,

$$I = (I_1 + I_2)/2. \tag{23}$$

2.4 Estimation of Intensities of Light Sources

In section 2.2, besides the specular image, we also generate a Lambertian image. The Lambertian intensity of each point on the sphere surface is highly relative to the directions and intensities of the light sources. The Lambertian intensity of any point (x, y, z) on the sphere surface can be written as:

$$I_{diffuse}(x, y, z) = Ia + \sum_{i=1}^{n} Id^{(i)}(N(x, y, z) \cdot L^{(i)}) \tag{24}$$

where

$$N(x, y, z) = \begin{pmatrix} x - s_x \\ y - s_y \\ z - s_z \end{pmatrix}. \tag{25}$$

N is the normal vector and $L^{(i)}$ is the light direction vector of the i'th light source. Ia is the ambient intensity, and $Id^{(i)}$ is the illumination intensity contributed by the i'th light source. For every pixel (i_1, j_1) in the image, we can find the corresponding point (x, y, z) on the sphere surface, then the Lambertian intensity of a pixel (i_1, j_1) in the image is:

$$I_{diffuse}(i_1, j_1) = Ia + \sum_{i=1}^{n} Id^{(i)}(N(i_1, j_1) \cdot L^{(i)}). \tag{26}$$

Since (s_x, s_y, s_z) is known, by equation (25), $N(i_1, j_1)$ can be calculated . Then equation (26) has $(i + 1)$ unknowns: Ia and $Id^{(i)}$. Applying equation (26) to every point in the Lambertian image, we get a error function:

$$EOF_3 = \sum_{(i_1, j_1)} [I_{diffuse}(i_1, j_1) - Ia - \sum_{i=1}^{n} Id^{(i)}(N(i_1, j_1) \cdot L^{(i)})]^2. \tag{27}$$

The remaining problem is how to minimize the error function (27) to get the $(i + 1)$ unknowns. We know that for such a minimization problem, the initial values and search range of the unknowns is crucial for the convergence and accurate results. We can restrict the search range and achieve better convergence

by observing that the intensities should be positive, i.e. Ia and $Id^{(i)}$ should be greater than zero. Based on this, we define a penalty function as

$$Intensity_{penalty} = \begin{cases} 0 & if Ia > 0 \; and \; Id^{(i)} > 0 \\ 10000 & otherwise \end{cases}$$

Combine the penalty function with the error function (27), we get:

$$EOF_4 = EOF_3 + intensity_{penalty}. \tag{28}$$

Minimizing above error function will give us the intensities of the light sources. The Levenberg-Marquardt non-linear optimization method is utilized to accomplish this task.

3 Experiments

3.1 Synthetic Images

In order to test the applicability of our algorithm, we have performed experiments on synthetic images of a sphere with three or more light sources. Since the ground truth is known, we can quantitatively evaluate the system. All the original images are synthesized using 256 grey levels, and light directions are represented as vectors in the camera coordinate system. The deviations of the estimated light directions and intensities from the true light directions and intensities are calculated to estimate the accuracy of the system.

In separating the image into Lambertian and specular images, the appropriate values should be choosen for parameters $th_{Lambertian}$ and $th_{specular}$. For $th_{Lambertian}$, choosing a small value means that in order to be a diffuse pixel, the difference of intensities between the corresponding pixels in the right and left image should be small, and it also means that the intensities of the diffuse pixels should have less noise to satisfy the situation. The tradeoff is that the number of candidate pixels will be reduced. For $th_{specular}$, choosing a larger value means that in order to be a specular pixel, the difference of intensities between the corresponding pixels in the right and left image should be larger, which would result in a smaller specular spot and eliminate the overlap problem, but it could also result in some specular spot disappearance when some inappropriate large value is chosen. Figure 5 shows a image pair with 6 light sources being separated with different $th_{specular}$. Figure 5c uses a smaller value which has the overlap problem, while 5d uses a larger value, where the overlap problem has been resolved.

Figure 6 shows an experiment result on 48 different light sources. The angles between various light directions and x axis ranges from 30^o to 120^o. Figure 6a shows the error distribution of light directions, 6b shows the error distribution of light intensities. As seen from the figure, the average error in estimated directions is about 0.3^o, the average error of estimated intensity is about 3%.

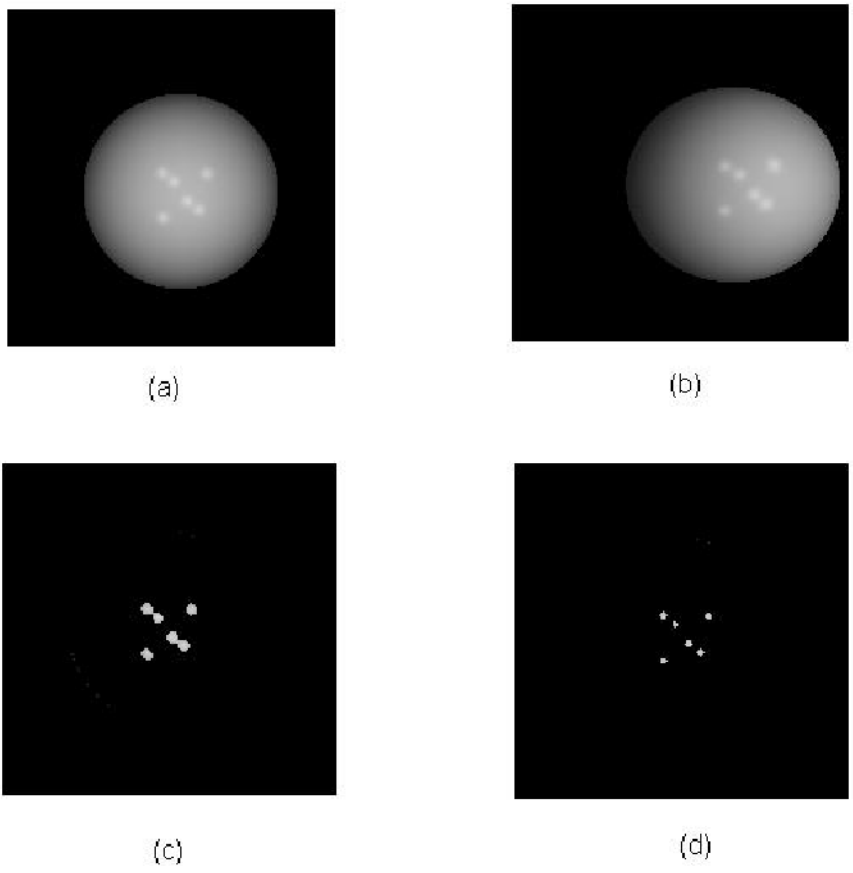

Fig. 5. (a) Right image, (b) left image, (c) specular image using a small $threshold_{specular}$, (d) specular image using a larger $threshold_{specular}$

3.2 Real Images

In order to test and evaluate our approach in practice, we have performed experiments with real images. Figure 8 shows a pair of real images of a plastic sphere illuminated with two light sources. The images were acquired with Trinocular stereo (Triclops) system: a 3-eye stereo camera designed by PointGrey Inc. This device provides us rectified image and camera calibration parameters. The picture is taken with a black cloth as the background to facilitate thresholding of the sphere.

Forty light sources with different directions and intensities in total were used to create different kinds of images. The directions of the light sources were manually measured as ground truth. As shown in figure 7, the average error of estimated directions is about 3^o.

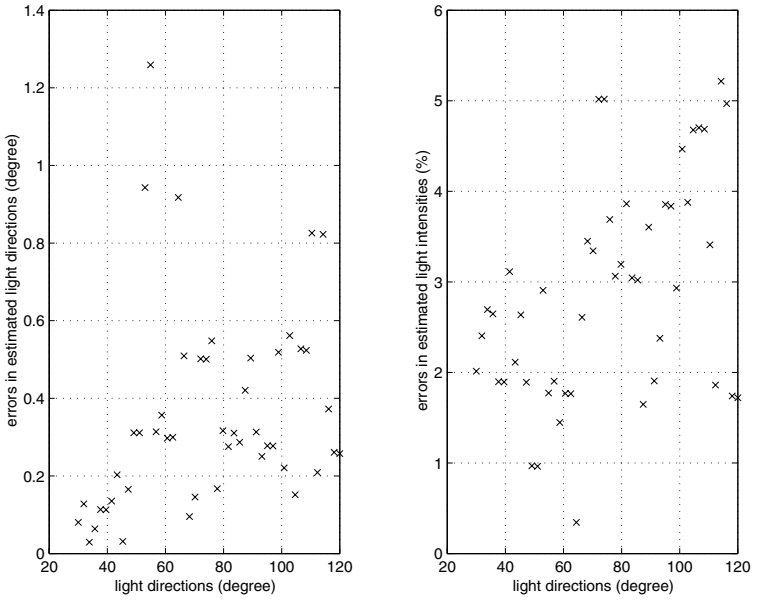

Fig. 6. Error estimation for synthetic image

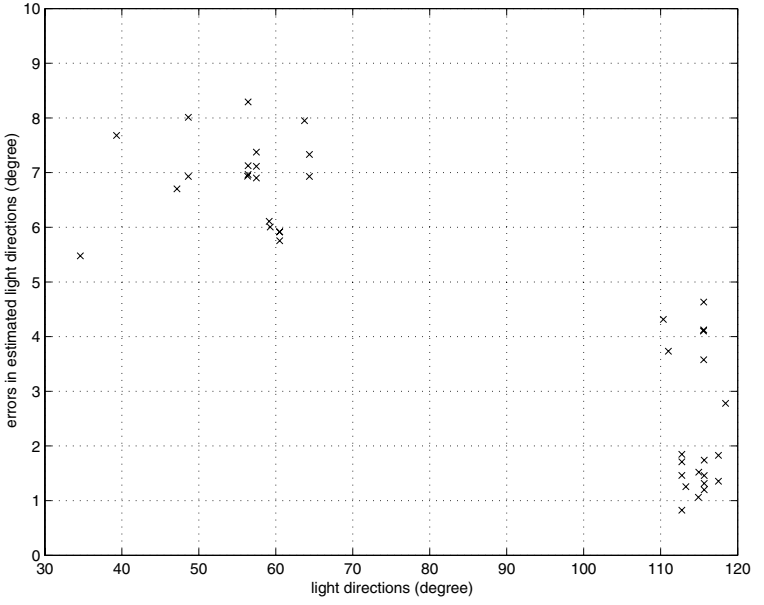

Fig. 7. Error estimation for real image

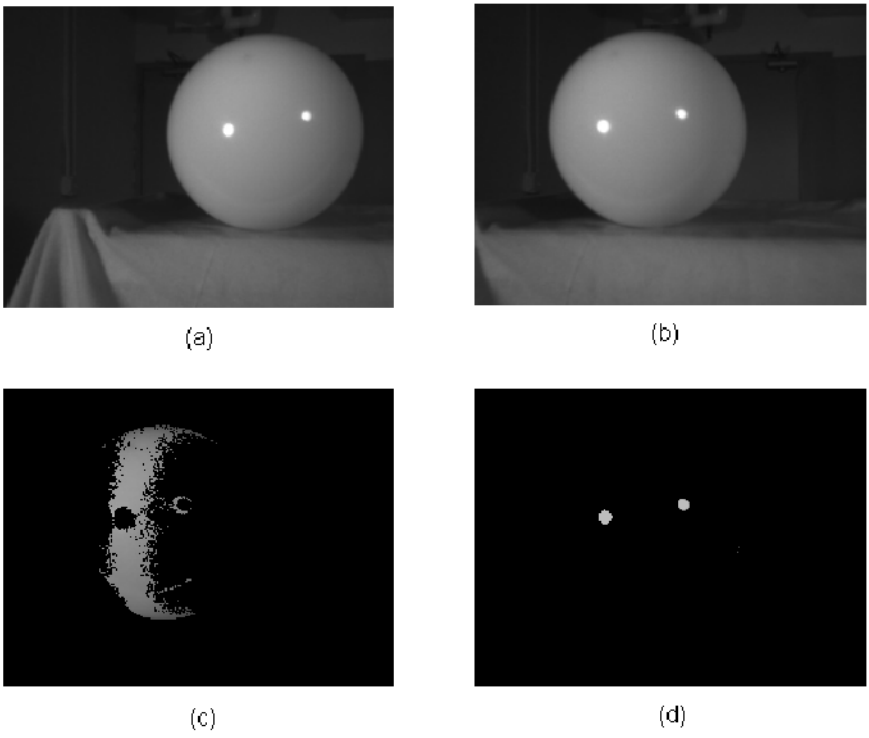

Fig. 8. Real image pair

From Figure 7, we can see that the errors of different direction regions have different error ranges. This is plausible, since the algorithm treats the sphere as an ideal sphere, and uses this ideal sphere model to get the normal and reflection vectors of the specular points on the sphere surface. In our experiments, the sphere is not an ideal one, different parts of the sphere have different pits and bumps, which result in different errors in estimating the light sources in different parts. We can expect better results if more ideal sphere is used.

The estimated light intensities are used to reconstruct the sphere images together with the directions information. Figure 9 shows a real image and a reconstructed synthetic image. Note that the two images look identical.

4 Conclusion and Future Work

This paper presents a novel scheme for locating multiple light sources and estimating their intensities from a pair of stereo images of a sphere, without the prior knowledge of the location and radius of the sphere. Unlike previous works in the area, the sphere surface is not assumed to be a pure Lambertian surface, instead, it has both Lambertian and specular properties. Experiment results on

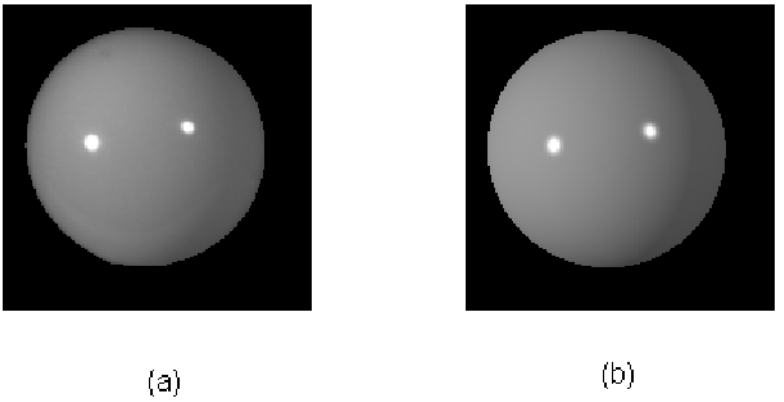

Fig. 9. (a) Real image; (b) reconstructed image

both synthetic and real images show that our algorithm works very well in tracking the locations of multiple light sources. Main advantage of this algorithm is that the knowledge of location and size of the sphere is not necessary, which gives more flexibility to apply it in practical situations. Another advantage is that besides the locations of the light sources, it can also recover the intensity information of the light sources, which is very useful in 'mixing' the synthetic imagery into a real scene. Future work includes extensions of the method to objects other than spheres, and applying the illumination information to enhance shape from shading algorithms.

References

1. Q.Zheng, R.Chellappa: Estimation of Illumination, Albedo, and Shape from Shading. IEEE Trans. Pattern. Anal. Mach. Intell. **13** (1991) 680–702.
2. C. H. Lee and A. Rosenfeld: Improved Methods of Estimating Shape from shading Using the Light Source Coordinate System. Artificial Intelligence No. 26 (1985) 125–143
3. A. Pentland: Linear shape from shading. IJCV, Vol.4 (1990) 153–162
4. K. Ikeuchi and K. Sato: Determining reflectance parameters using range and brightness images. Proc 3rd IEEE ICCV, (1990) 12–20
5. M. J. Brooks and B. K. P. Horn: Shape and Source from Shading. Proceedings of the 9th International Joint Conference on Artificial Intelligence. (1985) 932–936
6. W. Chojnacki, M. J. Brooks and D. Gibbins: Revisiting Pentland's Estimator of Light Source Direction. J. Opt. Soc. Am. A, Vol.11, No.1, (1994) 118–124
7. Y.Zhang, Y.Yang: Illumination Direction Determination for Multiple Light Sources. CVPR, vol.1, (2000) 269–276
8. R.C. Gonzalez and P. Wintz: Digital Image Processing. Addison-Wesley Publishing Company, Inc, 1977

9. A. P. Pentland: Finding the Illuminant Direction. J. Opt. Soc. Am. 72, (1982) 448–455
10. T. A.Mancini and L. B. Wolff: 3D shape and light source location from depth and reflectance. IEEE CVPR, (1992) 707-709
11. D. R. Hougen and Narendra. Ahuja: Estimation of the light source distribution and its use in integrated shape recovery from stereo and shading. Proc 4th IEEE ICCV (1993) 148–155
12. Donald. Hearn and M. Pauline. Baker: Computer graphics Prentice Hall, 1997
13. Y. Yang and A. Yuille: Source from shading. IEEE CVPR (1991) 534–539
14. M.W.Powell, D.Goldgof: Calibration of Light Sources. CVPR, vol.2, (2000) 263–269
15. M.W.Powell, S.Sarkar, D.Goldgof: A Simple Strategy for Calibrating the Geometry of Light Sources. IEEE transaction on PAMI vol.23, No. 9 (september 2001) 1022-1027